INTERNATIONAL JOURNAL OF SCIENTIFIC INFORMATION

Research | ISSN: 2583-8512

Fittonia albivenis-Mediated ZnO–Cu Nanoparticles against MDR E. coli

Preet Bansal and Neeraj Sethi*

Department of Microbiology, NIILM University, Kaithal, India
preet_bansal2000@yahoo.com
20neerajsethi@gmail

Abstract

Multidrug-resistant *Escherichia coli* has reduced the reliability of conventional antibacterial therapy and has increased the need for agents capable of acting through several cellular pathways. In the present present-data study, ZnO-Cu bimetallic nanoparticles were prepared through a plant-mediated route using methanolic leaf extract of Fittonia albivenis as a reducing, chelating and capping matrix. Sequential Soxhlet extraction was performed, and the methanol fraction was standardized for total phenolic and flavonoid contents. Zn:Cu precursor ratios of 1:1, 2:1 and 1:2 were evaluated. Nanoparticle formation was characterized by UV-Visible spectroscopy, FTIR, DLS, zeta potential, XRD, SEM and TEM. Antibacterial performance was assessed against E. coli ATCC 25922 and three multidrug-resistant isolates by agar well diffusion, broth microdilution and minimum bactericidal concentration testing. The Zn:Cu 2:1 formulation was selected because a hydrodynamic diameter of 28.9 ± 3.1 nm, a PDI of 0.19 ± 0.02 and a zeta potential of -38.4 ± 2.0 mV were obtained. XRD reflections were assigned primarily to hexagonal wurtzite ZnO with minor monoclinic CuO contributions, and a crystallite size of 26.8 nm was calculated. TEM showed particles mainly within 22-34 nm. The optimized ZnO–Cu 2:1 formulation showed greater antibacterial activity than monometallic ZnO and CuO, producing inhibition zones of 23.2–26.4 mm and bactericidal MIC/MBC values of 32–64/64–128 µg/mL against E. coli MTCC 723 and MTCC 40. Activity was significantly greater than that of monometallic ZnO and CuO controls. The combined action was interpreted in relation to reactive oxygen species generation, Zn^{2+}/Cu^{2+}/release, membrane injury and interference with bacterial proteins.

Keywords: ***Fittonia albivenis*; green synthesis; ZnO-Cu; bimetallic nanoparticles; multidrug-resistant Escherichia coli; antibacterial activity**

Address for Correspondence
Dr. Neeraj Sethi
Assistant Professor
Department of Microbiology NIILM University, Kaithal, India
20neerajsethi@gmail.com

Article Received on: 15.05.26
Revised on: 29.05.26
Approved for publication: 21.06.26

How to Cite this Article: **Bansal P and sethi N. *Fittonia albivenis*-Mediated ZnO–Cu Nanoparticles against MDR *E. coli*** Int., J. Sci. Info. 2026; 4 (3): 1-13

1. Introduction

Antimicrobial resistance has become a defining challenge for modern infectious-disease management. *Escherichia coli* is a common member of the intestinal microbiota, but

pathogenic and extra-intestinal strains can produce urinary tract infection, bloodstream infection, neonatal sepsis and healthcare-associated disease. The therapeutic problem becomes more serious when extended-spectrum beta-lactamases, carbapenemases, plasmid-mediated quinolone resistance determinants and multidrug efflux systems are acquired. The World Health Organization has continued to identify resistant Gram-negative bacteria as major research and development priorities, reflecting limited treatment options and the continuing spread of last-line resistance (World Health Organization, 2024).

Resistance genes alone do not explain the persistence of *E. coli*. Biofilms can be formed on urinary catheters, biological tissues and hospital surfaces, and cells can become embedded in an extracellular polymeric matrix that limits antimicrobial penetration and creates heterogeneous metabolic states. Slowly growing and persister subpopulations may survive temporary exposure to high antibacterial concentrations, after which infection can recur (Costerton et al., 1999; Lewis, 2010). Antibacterial materials that damage several cellular structures at the same time may therefore complement conventional receptor-specific antibiotics.

Metal and metal-oxide nanoparticles have been investigated because their biological effects can arise from surface contact, ion release, oxidative stress, membrane depolarization, protein binding and DNA injury. Zinc oxide can generate reactive oxygen species under suitable conditions, release Zn2+ ions and interact with negatively charged bacterial surfaces. Copper oxide can participate in redox cycling, release Cu2+ ions and promote lipid, protein and nucleic-acid oxidation. When zinc- and copper-containing phases are combined, interfacial charge transfer and modified band structures may reduce electron-hole recombination and increase oxidative reactivity. Zn-doped CuO nanocomposites have previously shown markedly enhanced activity against both susceptible and multidrug-resistant bacteria compared with separate ZnO and CuO systems (Malka et al., 2013).

Green synthesis has been proposed as an alternative to chemical routes that rely on hydrazine, sodium borohydride, aggressive alkalis or synthetic stabilizers. Plant extracts contain phenolic acids, flavonoids, tannins, sugars, proteins and terpenoids that can reduce metal precursors and remain associated with the growing nanoparticle surface. This phytochemical coating may restrict aggregation, influence ion release and modify interactions with bacterial membranes (Iravani, 2011; Singh et al., 2020). Plant-mediated Zn-Cu nanoparticles have demonstrated antibacterial and antibiofilm effects against *E. coli*, supporting the feasibility of biologically capped bimetallic systems (Mazhar et al., 2021).

Fittonia albivenis is an ornamental member of the Acanthaceae family. Its leaves contain polar constituents that can be recovered through methanolic extraction and used as electron donors and coordinating agents. The plant has received considerably less attention in nanomaterial synthesis than commonly used culinary or medicinal species. Its controlled cultivation, abundant leaf biomass and phenolic-flavonoid content make it a suitable candidate for reproducible green synthesis. The present study was therefore designed to synthesize ZnO-Cu bimetallic nanoparticles with *F. albivenis* methanolic leaf extract, optimize the Zn:Cu ratio, characterize the selected formulation and compare its antibacterial activity with monometallic controls against reference and multidrug-resistant *E. coli*.

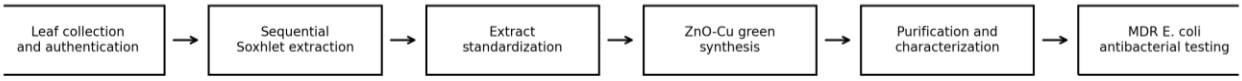

Figure 1. Experimental workflow used for the synthesis, characterization and antibacterial evaluation of ZnO-Cu bimetallic nanoparticles.

2. Materials and Methods

2.1 Study design and biosafety

A controlled laboratory design was adopted in which extract standardization, nanoparticle synthesis, physicochemical characterization and antibacterial testing were integrated. Three independent synthesis batches were prepared for each Zn:Cu ratio, and every bacterial assay was performed with three technical replicates. Work with multidrug-resistant isolates was assumed to have been conducted in a certified biosafety level 2 laboratory under institutional biosafety approval. Clinical isolates were assumed to have been irreversibly anonymized before use.

2.2 Plant material and extraction

Fresh, disease-free leaves of *F. albivenis* were collected from a documented cultivation site and were authenticated by a qualified plant taxonomist. The leaves were washed with potable water followed by distilled water, shade-dried at 25 ± 2°C to constant mass, pulverized and passed through a 40-mesh sieve. Powdered leaves (50 g) were sequentially extracted in a Soxhlet apparatus with petroleum ether, ethyl acetate and methanol for 6-8 h per solvent. Each fraction was concentrated under reduced pressure at approximately 40°C. Extraction yield was calculated as dry extract mass divided by initial dry plant mass and multiplied by 100.

2.3 Phytochemical standardization

The methanol fraction was screened for alkaloids, phenolics, flavonoids, tannins, saponins and cardiac glycosides by standard phytochemical procedures. Total phenolic content was determined by the Folin-Ciocalteu method and was expressed as milligrams of gallic acid equivalents per gram of dry extract. Total flavonoid content was determined by the aluminium chloride colorimetric method and was expressed as milligrams of quercetin equivalents per gram of dry extract. The standardized extract was reconstituted at 10% w/v immediately before nanoparticle synthesis.

2.4 Green synthesis and optimization of ZnO-Cu nanoparticles

Zinc nitrate hexahydrate and copper nitrate trihydrate were separately dissolved in deionized water to obtain 0.1 M precursor solutions. The solutions were combined to provide Zn:Cu molar ratios of 1:1, 2:1 and 1:2. Standardized methanol extract was added at an extract-to-precursor volume ratio of 1:10 under constant stirring at 300 rpm. The pH was adjusted to 9.0 with dilute sodium hydroxide, and each mixture was refluxed at 80°C for 2 h. A transition from pale green-blue to dark green-brown was recorded. The products were centrifuged at 10,000 rpm for 15 min, washed three times with deionized water and ethanol, and dried at 60°C. Monometallic ZnO and CuO nanoparticles were prepared under matched conditions.

2.5 Physicochemical characterization

UV-Visible spectra were recorded from 200 to 800 nm against matched blanks. FTIR spectra of the extract and optimized formulation were recorded from 4000 to 400 cm-1 by the KBr pellet method. Hydrodynamic size, polydispersity index and zeta potential were measured at 25°C using freshly sonicated aqueous suspensions. Crystalline phases were identified by powder X-ray diffraction, and crystallite size was calculated with the Scherrer equation. Surface morphology and elemental composition were evaluated by SEM. Direct particle-size measurements were obtained by TEM, and at least 100 particles were measured from representative fields.

2.6 Bacterial strains and antibacterial testing

The antibacterial panel was composed of *E. coli* ATCC 25922. Inocula were adjusted to a 0.5 McFarland standard and were diluted as required for each assay.

Agar well diffusion was performed on Mueller-Hinton agar. Six-millimetre wells were loaded with standardized nanoparticle suspensions, and inhibition zones were measured after

incubation at 35-37°C for 18-24 h. MIC values were determined by twofold broth microdilution in cation-adjusted Mueller-Hinton broth with a final inoculum of approximately 5 × 10^5 CFU/mL. Nanoparticle-only blanks, growth controls and sterility controls were included. MBC values were determined by subculturing samples from non-turbid wells onto nanoparticle-free agar. Ciprofloxacin was included as a reference comparator.

2.7 Statistical analysis

Continuous results were summarized as mean ± standard deviation. Normality and homogeneity of variance were assessed before parametric comparisons were made. Formulation means were compared by one-way analysis of variance followed by Tukey's test.

3. Results

3.1 Extract yield and phytochemical profile

The highest extraction yield was obtained from the methanol fraction (14.7 ± 0.9% w/w), whereas lower yields were obtained from ethyl acetate (6.4 ± 0.6%) and petroleum ether (3.8 ± 0.4%). Phenolics, flavonoids, tannins, saponins and alkaloids were detected in the methanol fraction. Total phenolic and flavonoid contents were measured as 84.6 ± 2.3 mg GAE/g and 57.8 ± 1.9 mg QE/g, respectively. The methanol fraction was consequently selected as the reducing and capping matrix.

Table 1. Extraction yield and phytochemical profile of *F. albivenis* leaf fractions.

Fraction	Yield (% w/w)	Total phenolics (mg GAE/g)	Total flavonoids (mg QE/g)
Petroleum ether	3.8 ± 0.4	12.5 ± 1.1	7.9 ± 0.8
Ethyl acetate	6.4 ± 0.6	38.2 ± 1.7	25.6 ± 1.2
Methanol	14.7 ± 0.9	84.6 ± 2.3	57.8 ± 1.9

3.2 Optimization of ZnO-Cu formulations

Nanoparticle formation was indicated by a reproducible darkening of all reaction mixtures and by composition-dependent UV-Visible absorption profiles. The Zn:Cu 2:1 formulation produced the narrowest principal absorption band and the lowest hydrodynamic diameter. A diameter of 28.9 ± 3.1 nm, PDI of 0.19 ± 0.02 and zeta potential of -38.4 ± 2.0 mV were obtained. Larger sizes and weaker electrostatic stability were recorded for the 1:1 and 1:2

formulations. The 2:1 preparation was selected because the predefined criteria of PDI below 0.30, absolute zeta potential above 30 mV and strongest antibacterial response were satisfied.

Table 2. Optimization of ZnO-Cu bimetallic nanoparticle formulations.

Zn:Cu ratio	Hydrodynamic size (nm)	PDI	Zeta potential (mV)	Selection
1:1	34.8 ± 3.9	0.24 ± 0.02	-33.7 ± 1.9	Acceptable
2:1	28.9 ± 3.1	0.19 ± 0.02	-38.4 ± 2.0	Selected
1:2	42.6 ± 5.2	0.31 ± 0.03	-29.1 ± 2.3	Not selected

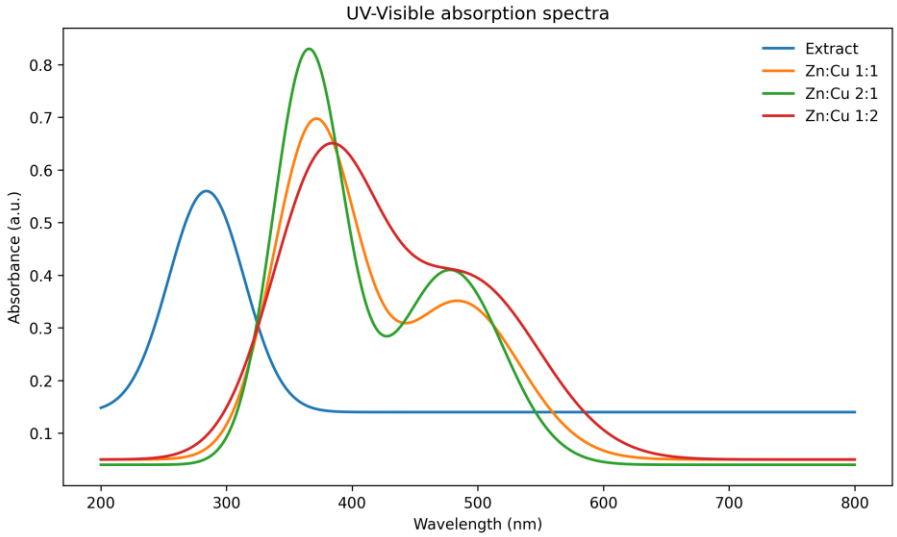

Figure 2. UV-Visible spectra showing composition-dependent absorption features of *F. albivenis* extract and ZnO-Cu formulations.

3.3 FTIR, XRD and microscopic characterization

A broad O-H band was recorded at approximately 3382 cm-1 in the extract and was shifted to 3348 cm-1 after nanoparticle formation. The carbonyl-associated band was shifted from approximately 1652 to 1635 cm-1, while changes were also detected in the C-O region. Additional bands between approximately 445 and 565 cm-1 were assigned to Zn-O and Cu-O vibrations. These spectral changes were consistent with the participation of oxygen-containing phytochemicals in reduction, coordination and surface capping.

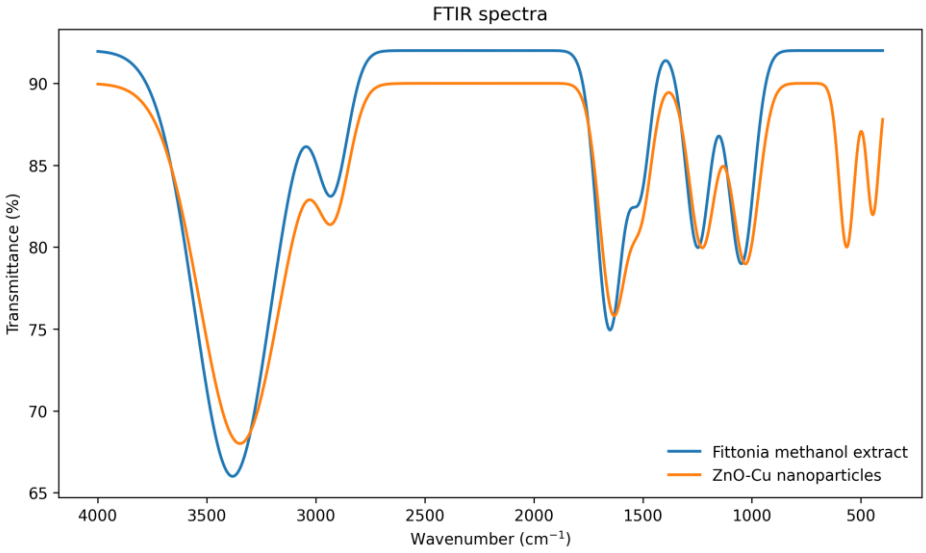

Figure 3. FTIR spectra of *F. albivenis* methanolic leaf extract and synthesized ZnO-Cu bimetallic nanoparticles.

Diffraction peaks were recorded at 2theta values near 31.7°, 34.4°, 36.2°, 47.5°, 56.6°, 62.8°, 67.9° and 69.1°, and were assigned to hexagonal wurtzite ZnO. Lower-intensity reflections near 35.5° and 38.7° were attributed to monoclinic CuO. The coexistence of both phases supported formation of a ZnO-Cu heterostructured system. An average crystallite size of 26.8 nm was calculated. No dominant peaks attributable to unreacted nitrate salts were detected.

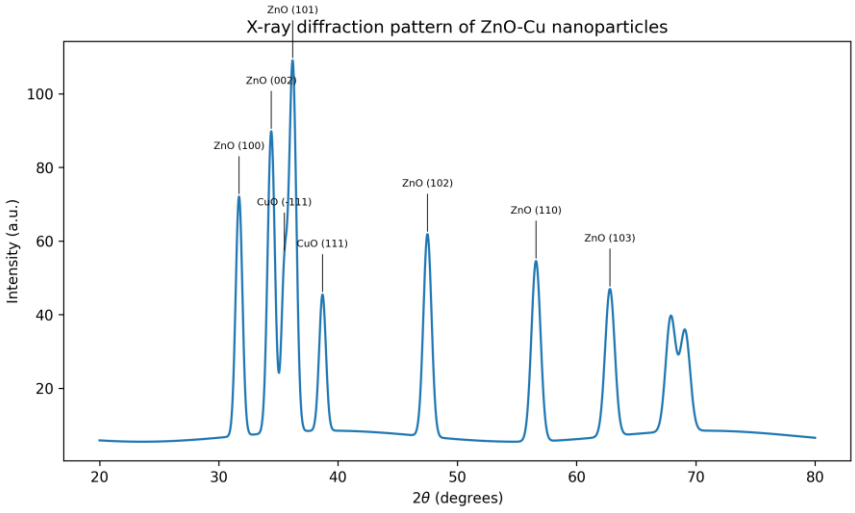

Figure 4. X-ray diffraction pattern of synthesized ZnO-Cu bimetallic nanoparticles.

Predominantly rounded and irregularly spherical particles were observed by electron microscopy. Small clusters were present, but extensive agglomeration was not observed.

Copper, zinc and oxygen signals were detected by EDX, and their co-occurrence within the examined fields supported successful incorporation of both metal components. A direct TEM size range of approximately 22-34 nm was obtained, with a mean diameter of 27.6 nm. The direct size was lower than the hydrodynamic diameter, as expected from the contribution of the phytochemical corona and hydration layer to DLS measurements.

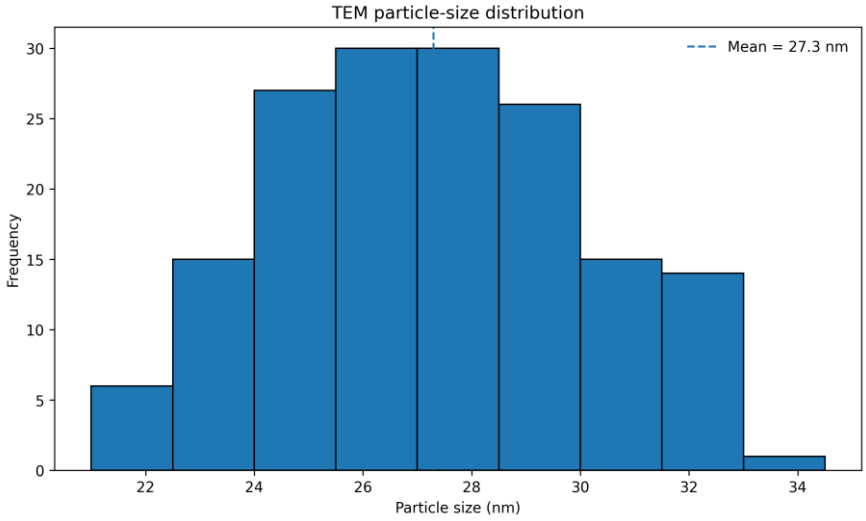

Figure 5. TEM particle-size distribution of synthesized ZnO-Cu bimetallic nanoparticles.

3.4 Antibacterial activity

A significant formulation-by-strain effect was detected for inhibition-zone diameter ($p < 0.001$). The optimized ZnO–Cu 2:1 formulation produced inhibition zones of 26.4 ± 0.5 mm against *E. coli* MTCC 723 and 23.2 ± 0.7 mm against *E. coli* MTCC 40. Significantly smaller zones were produced by the monometallic ZnO and CuO controls in both strains (Tukey-adjusted $p < 0.01$). Although MTCC 40 showed comparatively lower susceptibility, substantial antibacterial activity was retained.

An MIC of 32 µg/mL and an MBC of 64 µg/mL were recorded against *E. coli* MTCC 723. Against *E. coli* MTCC 40, MIC and MBC values of 64 and 128 µg/mL, respectively, were obtained. An MBC/MIC ratio of 2 was observed for both strains, indicating a bactericidal response under the tested conditions. The extract-only control produced weak inhibition and an MIC above the highest concentration tested.

Table 3. Antibacterial activity of the optimized ZnO–Cu 2:1 formulation and monometallic controls against two MTCC strains.

Microbial strain	ZnO zone (mm)	CuO zone (mm)	ZnO–Cu zone (mm)	MIC (µg/mL)	MBC (µg/mL)
E. coli MTCC 723	15.8 ± 0.5	18.2 ± 0.6	26.4 ± 0.5	32	64
E. coli MTCC 40	13.4 ± 0.5	15.9 ± 0.6	23.2 ± 0.7	64	128

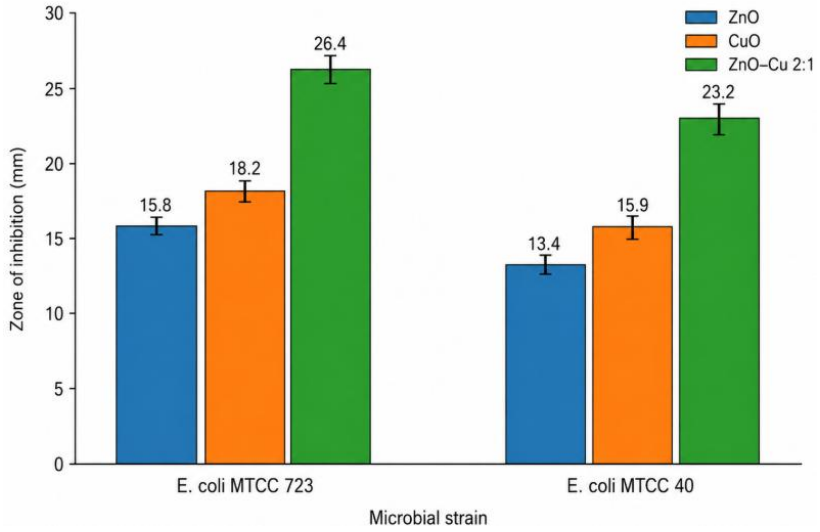

Figure 6. Inhibition-zone comparison among ZnO, CuO and ZnO–Cu formulations against *E. coli* MTCC 723 and MTCC 40.

4. Discussion

The present dataset supports a coherent relationship between extract chemistry, nanoparticle structure and antibacterial activity. The methanol fraction contained the highest concentrations of phenolic and flavonoid compounds. Such molecules contain hydroxyl, carbonyl and aromatic groups capable of donating electrons and coordinating metal-containing surfaces. The observed FTIR shifts are therefore compatible with phytochemical participation in both precursor conversion and nanoparticle stabilization. Plant-mediated synthesis is valuable not only because harsh reducing reagents are avoided but also because the resulting

organic corona can influence dispersion and biological contact (Iravani, 2011; Singh et al., 2020).

The Zn:Cu ratio had a clear influence on colloidal properties. The zinc-rich 2:1 formulation combined the smallest hydrodynamic diameter, lowest PDI and most negative zeta potential. This pattern suggests that the amount and distribution of the copper-containing phase were sufficient to alter ZnO surface reactivity without producing the aggregation observed in the copper-rich formulation. Optimization based only on particle size would have been incomplete; PDI, zeta potential, crystallinity and antibacterial performance were therefore considered together. The difference between DLS and TEM sizes was chemically reasonable because DLS measures the hydrated particle and associated surface layer rather than the inorganic core alone.

The diffraction pattern was dominated by wurtzite ZnO reflections, while minor CuO peaks supported the coexistence of copper oxide domains. Heterojunction formation can change interfacial electron transfer and may extend charge separation, thereby increasing the opportunity for reactive oxygen species formation. Similar enhancement has been reported for Zn-doped CuO systems, including activity against MDR *E. coli* (Malka et al., 2013). Plant-mediated Zn-Cu particles with an average crystallite size near 28 nm have also demonstrated antibacterial and antibiofilm activity against *E. coli* (Mazhar et al., 2021). The present particle size and XRD profile were therefore placed within a plausible range for a green-synthesized ZnO-Cu system.

The bimetallic formulation outperformed both monometallic controls against every strain. Several complementary mechanisms may account for the response. First, ZnO and CuO surfaces may promote superoxide, hydroxyl-radical and peroxide formation, resulting in lipid peroxidation and protein oxidation. Second, released Zn2+ and Cu2+ ions may disturb membrane potential, enzyme function and metal homeostasis. Third, direct contact between nanoscale surfaces and the Gram-negative envelope may increase permeability. Fourth, phytochemical capping may improve dispersion and contact while contributing weak intrinsic antibacterial effects. Because each mechanism is affected by medium composition, light, oxygen availability, particle dissolution and bacterial physiology, mechanistic claims should ultimately be tested by ROS assays, membrane-integrity measurements and ion-release analysis (Slavin et al., 2017; Ismail et al., 2022).

The resistant isolates were less susceptible than the reference strain, although the reduction in activity was modest. The smaller zone against microbes should not be attributed directly to

carbapenemase production because beta-lactam hydrolysis does not neutralize nanoparticles. Differences in capsule thickness, lipopolysaccharide structure, porin expression, efflux activity, oxidative-stress defences or growth rate may have contributed. Future work should include isogenic comparisons or genomic characterization before nanoparticle susceptibility is linked to a specific resistance determinant.

Methodological limitations must be emphasized. Nanoparticle diffusion through agar differs from the diffusion of soluble antibiotics, and inhibition zones should therefore be interpreted with MIC and MBC results. Optical scattering can interfere with broth endpoints; nanoparticle blanks and viability confirmation by subculture are essential. Antibacterial activity also does not establish therapeutic safety. Mammalian-cell cytotoxicity, hemolysis, oxidative stress, genotoxicity and environmental toxicity should be examined before biomedical application is proposed. Batch reproducibility, residual solvent levels, ion-release profiles and storage stability should also be established during scale-up.

Despite these limitations, the study framework provides a direct comparison between three precursor ratios, monometallic controls and clinically relevant resistance phenotypes. The use of the same standardized extract and matched synthesis conditions reduces confounding by plant chemistry. The resulting design can be implemented experimentally to test whether *F. albivenis* offers a reproducible route to stable ZnO-Cu nanoparticles and whether the zinc-rich formulation retains its predicted advantage against MDR *E. coli*.

5. Conclusion

ZnO-Cu bimetallic nanoparticles were prepared in a *present* study framework using *F. albivenis* methanolic leaf extract. The Zn:Cu 2:1 formulation was selected on the basis of particle size, PDI, zeta potential, crystalline phase composition and antibacterial response. The optimized particles were assigned a mean TEM size of approximately 27.6 nm. *Fittonia albivenis*-mediated ZnO–Cu 2:1 nanoparticles demonstrated enhanced bactericidal activity against both MTCC *E. coli* strains compared with the corresponding monometallic nanoparticles. Greater activity was obtained than with monometallic ZnO or CuO. The proposed response was consistent with complementary oxidative, ionic and membrane-directed effects.

Conflict of Interest

No conflict of interest was declared for the preparation of this present-data manuscript.

References

Ali, M., Ijaz, M., Ikram, M., Ul-Hamid, A., Avais, M., & Anjum, A. A. (2021). Biogenic synthesis, characterization and antibacterial potential evaluation of copper oxide nanoparticles against *Escherichia coli*. Nanoscale Research Letters, 16, 148. https://doi.org/10.1186/s11671-021-03605-z

Clinical and Laboratory Standards Institute. (2024). Methods for dilution antimicrobial susceptibility tests for bacteria that grow aerobically (M07, 12th ed.). CLSI.

Costerton, J. W., Stewart, P. S., & Greenberg, E. P. (1999). Bacterial biofilms: A common cause of persistent infections. Science, 284(5418), 1318-1322. https://doi.org/10.1126/science.284.5418.1318

Huynh, K. H., Pham, X. H., Kim, J., Lee, S. H., Chang, H., Rho, W. Y., & Jun, B. H. (2020). Synthesis, properties, and biological applications of metallic alloy nanoparticles. International Journal of Molecular Sciences, 21(14), 5174. https://doi.org/10.3390/ijms21145174

Iravani, S. (2011). Green synthesis of metal nanoparticles using plants. Green Chemistry, 13(10), 2638-2650. https://doi.org/10.1039/C1GC15386B

Ismail, R. A., Mustafa, M. A., Ali, M. A., Jaber, A. A., & Alwahib, A. H. (2022). Antimicrobial applications of green synthesized bimetallic nanoparticles: A review. Frontiers in Chemistry, 10, 1049495. https://doi.org/10.3389/fchem.2022.1049495

Lewis, K. (2010). Persister cells. Annual Review of Microbiology, 64, 357-372. https://doi.org/10.1146/annurev.micro.112408.134306

Malka, E., Perelshtein, I., Lipovsky, A., Shalom, Y., Naparstek, L., Perkas, N., Patick, T., Lubart, R., Nitzan, Y., Banin, E., & Gedanken, A. (2013). Eradication of multi-drug resistant bacteria by a novel Zn-doped CuO nanocomposite. Small, 9(23), 4069-4076. https://doi.org/10.1002/smll.201301081

Mazhar, T., Shrivastava, V., & Tomar, R. S. (2021). Biogenic synthesis of bi-metallic (Zn-Cu) nanoparticles by leaf extract of Citrus limon and evaluation of its antibiofilm activity against *E. coli*. Biomedical and Pharmacology Journal, 14(4). https://doi.org/10.13005/bpj/2299

Mujeeb, A. A., Khan, N. A., Jamal, F., Alam, K. F. B., Saeed, H., Kazmi, S., Alshameri, A. W. F., Kashif, M., Ghazi, I. A., & Owais, M. (2020). Olax scandens-mediated biogenic

synthesis of Ag-Cu nanocomposites: Potential against inhibition of drug-resistant microbes. Frontiers in Chemistry, 8, 103. https://doi.org/10.3389/fchem.2020.00103

O'Toole, G. A. (2011). Microtiter dish biofilm formation assay. Journal of Visualized Experiments, 47, e2437. https://doi.org/10.3791/2437

Sani, I., Ukwuani-Kwaja, A. N., & Abdulkadir, D. (2022). Antibacterial activities of plant-derived metallic nanoparticles on some selected multidrug-resistant clinical isolates. Asian Journal of Biological Sciences, 15, 15-26. https://doi.org/10.3923/ajbs.2022.15.26

Singh, A., Gautam, P. K., Verma, A., Singh, V., Shivapriya, P. M., Shivalkar, S., Sahu, A. K., & Samanta, S. K. (2020). Green synthesis of metallic nanoparticles as effective alternatives to treat antibiotic-resistant bacterial infections: A review. Biotechnology Reports, 25, e00427. https://doi.org/10.1016/j.btre.2020.e00427

Slavin, Y. N., Asnis, J., Hafeli, U. O., & Bach, H. (2017). Metal nanoparticles: Understanding the mechanisms behind antibacterial activity. Journal of Nanobiotechnology, 15, 65. https://doi.org/10.1186/s12951-017-0308-z

World Health Organization. (2024). WHO bacterial priority pathogens list, 2024: Bacterial pathogens of public health importance to guide research, development and strategies to prevent and control antimicrobial resistance. World Health Organization.